

1 **Anomalous incisor morphology indicates tissue-specific roles for *Tfap2a* and *Tfap2b* in**
2 **tooth development**

3 Emily D. Woodruff, Galaxy C. Gutierrez, Eric Van Otterloo, Trevor Williams, Martin J. Cohn

4
5 **Supplementary Materials**

6
7 **5. Supplementary Methods**

8 **5.1 Lineage tracing of *Sox10*-positive cranial neural crest cells**

9 ***CNCC lineage tracing:*** In *Sox10-iCre/ER^{T2}* embryos, *Cre*-mediated recombination is
10 driven by the *Sox10* promoter and is induced by tamoxifen. In the presence of tamoxifen, the
11 iCRE/ER^{T2} fusion protein binds tamoxifen and translocates to the nucleus where it recombines
12 with the *R26R^{mTmG}* transgene, resulting in excision of the tdTomato sequence and expression of
13 EGFP in *Sox10*-expressing CNCCs. Tamoxifen (Sigma-Aldrich T5648) was mixed with filtered
14 corn oil (40 mg tamoxifen per 1 ml corn oil) and incubated at 37°C for 1.5-2 hours prior to
15 administration. For both lineage tracing experiments, we administered one dose of tamoxifen
16 (200 mg tamoxifen/kg mouse weight) to pregnant female mice by oral gavage either on one
17 single day (experiment 1: E6.5, E7.5, or E8.5) or on three consecutive days (experiment 2: E6.5-
18 E8.5).

19 ***Embryo processing:*** E13.5 embryos were dissected, fixed briefly in 4% PFA for 1 hour
20 on ice in the dark, rinsed in PBS, and screened for EGFP and tdTomato fluorescence. EGFP-
21 positive (*Cre*-positive) and tdTomato-positive embryos were prepared for cryosectioning as
22 described above (Methods 2.3). Results reported are based on a minimum of 3 embryos for each
23 time point within each of these experiments. After sectioning, tissue sections were briefly fixed
24 in 4% PFA for 10 minutes, rinsed twice in PBS and mounted on slides using Fluoromount-G
25 fluorescent mounting medium (Southern Biotech) and covered with glass coverslips (Thermo
26 Fisher Scientific). Membrane fluorescence for EGFP and tdTomato was visualized in frontal
27 cryosections using a Zeiss LSM 710 confocal microscope.

28 ***Genotyping:*** To genotype embryos, cells were lysed in sodium hydroxide (25mM) at
29 95°C for 1 hour, neutralized with tris hydrochloride (40mM), and diluted to ~5ng/μl. PCR for
30 both *R26R^{mTmG}* and *Sox10-iCre/ER^{T2}* alleles was performed using primers specific to each

31 transgene (Supplementary table 1) using the following conditions: 95°C for 3 minutes, 95°C for
32 30 seconds, 64°C for 30 seconds, 72°C for 1 minute for 35 cycles.

33

34 **5.2 Tissue-specific conditional deletion of *Tfap2a* and *Tfap2b***

35 In double mutant embryos generated from the first cross (*i.e.*,
36 *Tfap2a^{lox/flox};Tfap2b^{lox/flox};Cre+*), deletion of *Tfap2a* and *Tfap2b* was strictly isolated to the
37 tissue of interest (*i.e.*, the *Cre*-positive tissue), whereas *Cre*-negative tissues retained *Tfap2a* and
38 *Tfap2b* function and were essentially ‘wild-type’ (Supplementary figure 1 A, B). In the second
39 cross, however, double mutant embryos (*i.e.*, *Tfap2a^{null/flox};Tfap2b^{null/flox};Cre+*) lacked both
40 copies of *Tfap2a* and *Tfap2b* in *Cre*-expressing cells but remained heterozygous for *Tfap2a* and
41 *Tfap2b* in the rest of the embryo (Supplementary figure 1 C, D). Embryos that were
42 heterozygous for both *Tfap2a* and *Tfap2b* conditional alleles (*i.e.*, *Tfap2a^{w^t/flox};Tfap2b^{w^t/flox};Cre+*)
43 were used as controls. All *Tfap2* mouse lines were initially maintained on a mixed 129/Black
44 Swiss background (Brewer et al., 2004) but they have since been outcrossed to Black Swiss
45 (strain code 492, Charles River).

46 For the experiments involving *Tfap2* mutant embryos, DNA was extracted by placing the
47 isolated tissue in DirectPCR Lysis Reagent (Viagen Biotech) plus 10 µg/ml proteinase K
48 (Roche), incubated overnight at 65°C, followed by heat inactivation at 85°C for 45 min. The
49 lysed product was then used directly in a PCR reaction using the Qiagen DNA polymerase kit,
50 including the optional Q Buffer solution (Qiagen).

51

52 **5.3 Cloning of RNA probes for *in situ* hybridization**

53 **Primer and probe design:** Oligonucleotide primers (Supplementary table 3) were
54 designed in Geneious (v6.1.8 or 10.0.9, Biomatters, Ltd) such that the resulting amplicon (DNA
55 template for the RNA probe) was from a single exon. To ensure that the probes were specific to
56 the genes of interest, we performed BLAST (Basic Local Alignment Search Tool) searches of
57 the NCBI database (<http://blast.ncbi.nlm.nih.gov/>).

58 **Cloning:** PCR products were visualized using gel electrophoresis. The PGem-T Easy
59 vector (Promega) or the Strataclone vector (Strataclone) were used to clone the target DNA
60 fragments. These vectors contain M13 forward and reverse priming sites and the following
61 priming sites and polymerase start sites that were utilized in downstream steps in this protocol:

62 T7 (both vectors), T3 (Strataclone vector), and Sp6 (PGem-T Easy vector). Amplicons were
63 ligated into the vector and cloned using NEB Turbo competent cells (New England Biolabs)
64 grown on plates containing Luria-Bertani (LB) broth medium with ampicillin and X-gal was
65 used for blue/white screening of bacterial colonies. Transformed bacterial colonies were grown
66 with agitation (7 hours at 300 RPM or 12 hours at 225 RPM) in Terrific Broth media containing
67 ampicillin. Cultures were purified using the GenElute Miniprep kit (Sigma Aldrich) and linear
68 inserts were obtained using PCR with M13 forward and reverse primers. PCR products were
69 purified using the Promega PCR and Gel Clean-Up kit (Promega) and gel electrophoresis was
70 used to verify that the cloned fragments were the correct size. We determined the orientation of
71 the target sequence within the plasmid and validated the identity of each target gene sequence by
72 Sanger sequencing. “Antisense” and “sense” DIG-labeled RNA probes were synthesized in a
73 transcription reaction using the appropriate polymerase (T7, T3, or Sp6 (Promega)), purified
74 using the RNA Mini Quick Spin Columns (Roche) and the concentration (ng/ μ l) of each probe
75 was measured using a Nanodrop spectrophotometer (Thermo Fisher Scientific).

76

77 **5.4 *In situ* hybridization on cryosections**

78 Steps were performed at room temperature unless noted. Cryosections were thawed
79 briefly, fixed in 4% PFA with PBS (10 min), washed twice in DEPC-treated PBS + 0.1% Triton-
80 X 100 (DEPC-PBST) and treated with proteinase K (5 μ g PK/ml PBST, 5 min). Tissue was then
81 washed with DEPC-PBST and fixed again in 4% PFA (5 min), followed by an acetylation wash
82 to increase the specificity of the ISH signal (Braissant and Wahli, 1998). Sections were incubated
83 in warm pre-hybridization solution at 65°C (1-2 hours). DIG-labeled “antisense” and “sense”
84 RNA probes were diluted to concentrations ranging from 0.2-0.5 μ g/ μ l in warm prehybridization
85 solution and 0.2-0.5ml of this solution was immediately applied to each slide. Slides were
86 incubated at 65°C overnight in a humid hybridization chamber.

87 Slides were rinsed in a series of saline-sodium citrate (SSC) solutions of decreasing
88 stringency at 65°C: 5X SSC, 2X SSC + formamide + 0.1% CHAPS, and 0.2X SSC + 0.1%
89 CHAPS. Slides were rinsed in KTB solution (50mM TrisHCl pH 7.5, 150mM NaCl, 10mM
90 KCl, 1% Triton X-100), blocked with 20% goat serum in KTB (2 hrs at 4°C), and incubated
91 overnight at 4°C in anti-DIG-AP antibody (Roche) diluted in blocking buffer (1:3,000). Multiple
92 KTB washes (30-45 min each) were performed to remove non-specifically bound antibody,

93 followed by washes with NTMT solution (100mM Tris HCl pH 9.5, 100mM NaCl, 50mM
94 MgCl₂, 0.1% Triton X-100). Sections were placed in NBT-BCIP coloring solution for multiple
95 days. When the coloring was complete, the slides were rinsed in KTBT, fixed in 4% PFA,
96 mounted with Dako glycergel aqueous mounting medium (Agilent Technologies) and covered
97 with glass coverslips (Thermo Fisher Scientific). Tissue sections were photographed on a Leica
98 microscope using Kohler illumination and any subsequent adjustments made to
99 brightness/contrast were performed in Adobe Photoshop CS6 (v13.0.6) on the entire image.

100

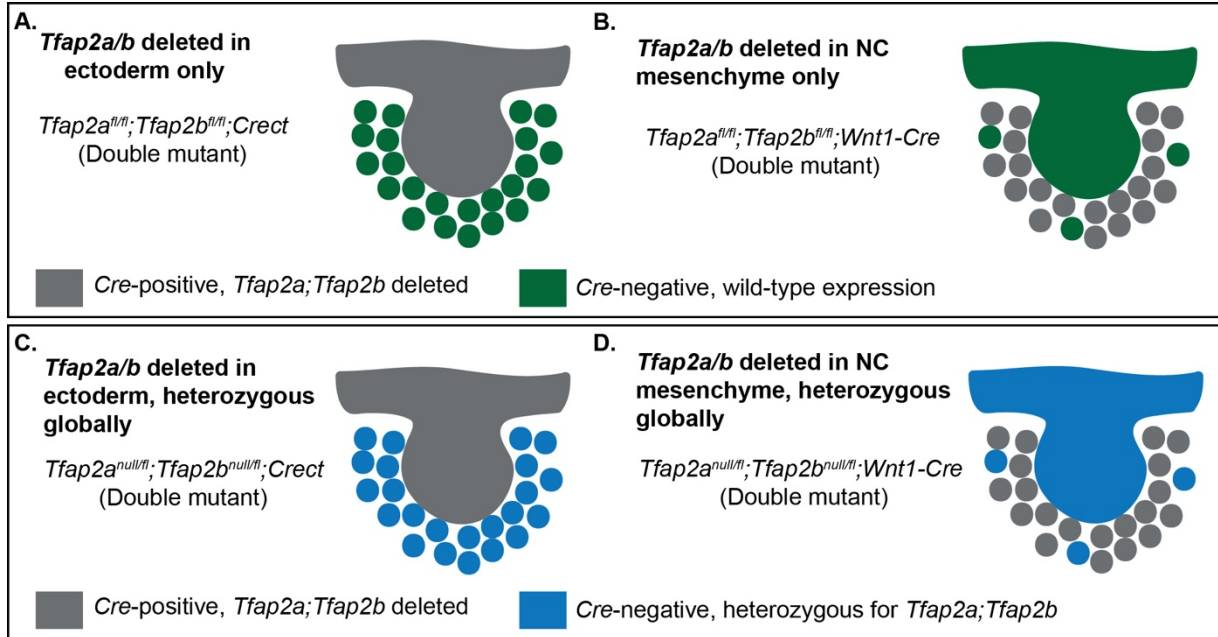
101 **5.5 Embryo processing for micro-CT scanning**

102 E18.5 embryos for micro-CT scanning were fixed in 4% PFA, rinsed in PBS, and stained
103 in the dark with a contrast-enhancing agent, Lugol's iodine solution (1.25% I₂, 2.5% KI with
104 DEPC water) overnight at room temperature. Excess iodine solution was removed with a Kim
105 Wipe and embryos were placed in a small plastic capsule to prevent desiccation during scanning.
106 After scanning, embryos were rinsed in 70% ethanol and then PBS to remove the iodine stain
107 and were subsequently processed for histological analysis as described above (see Methods 2.4).
108 Lugol's solution causes some degree of tissue shrinkage (Metscher, 2009), but we expect that
109 this shrinkage was similar across same-stage embryos because the duration in Lugol's was the
110 same for all embryos.

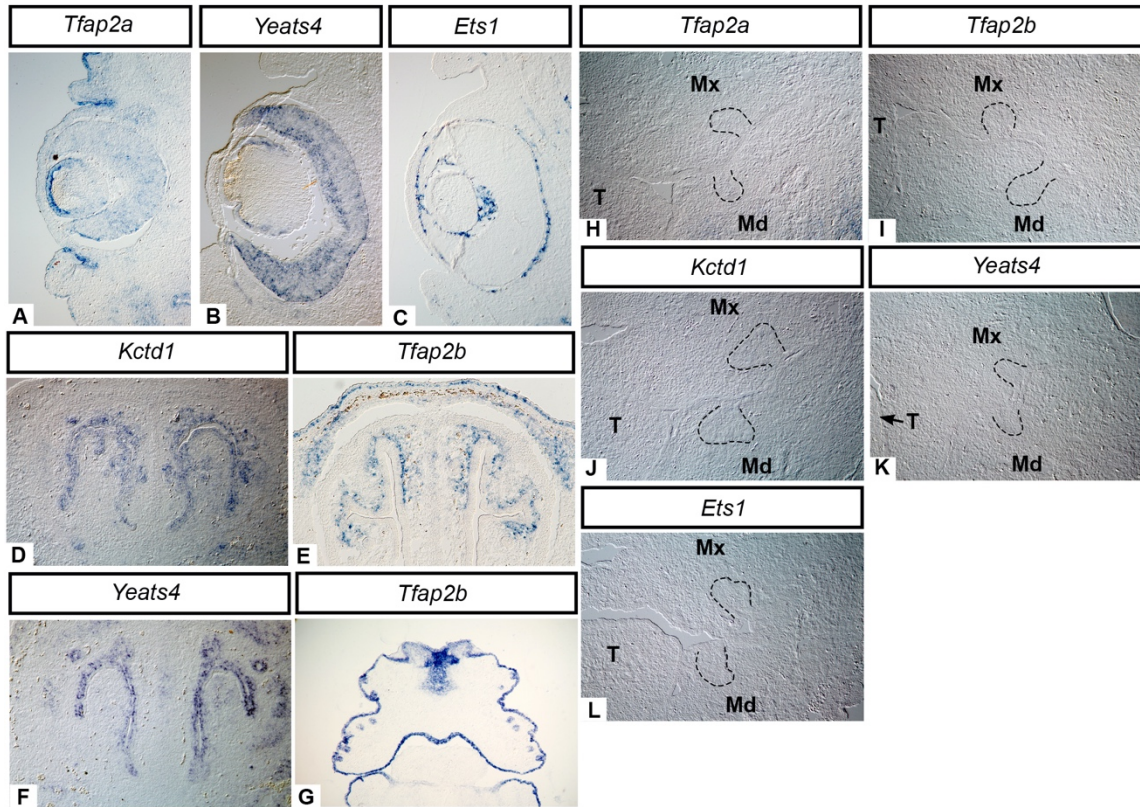
111

112

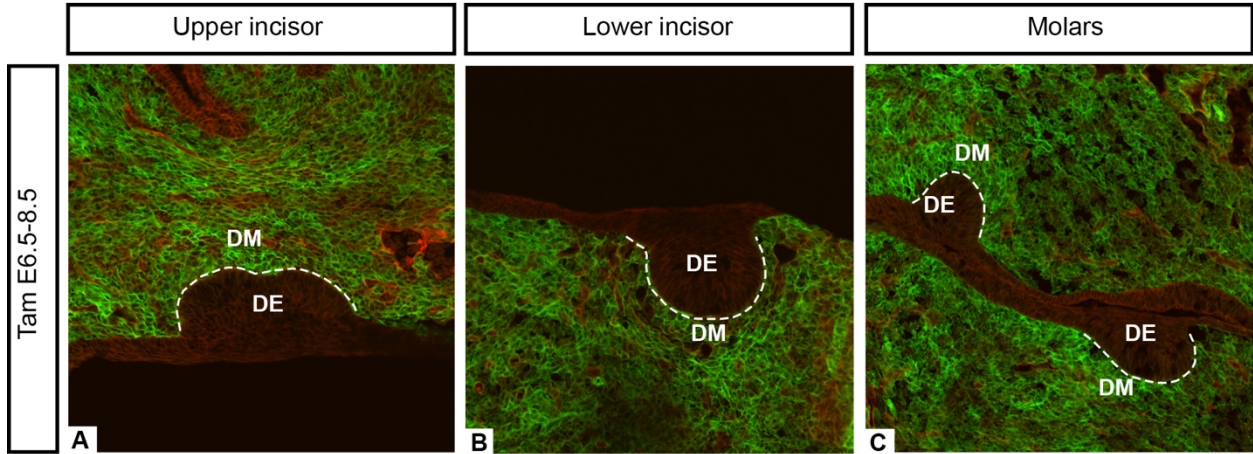
113 **Supplementary Figures and Tables**
 114



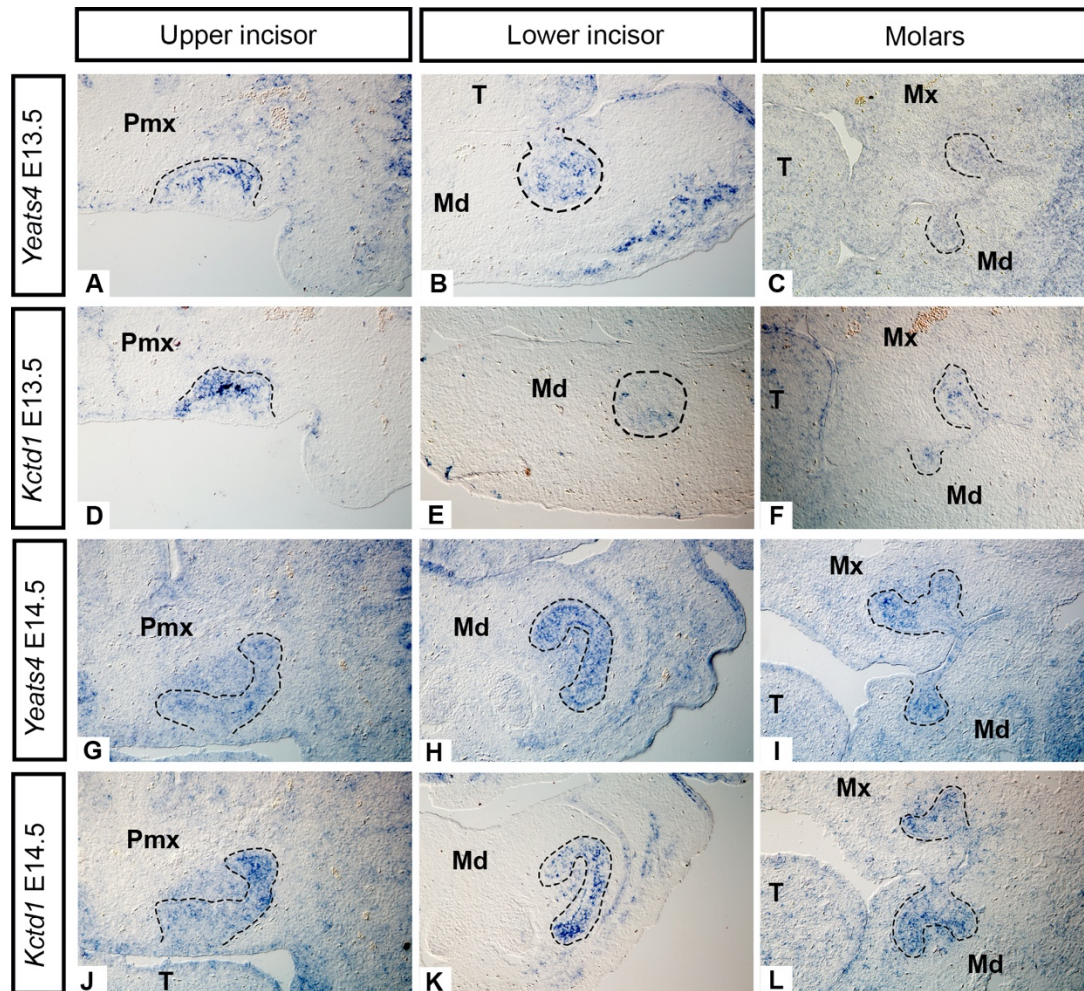
115
 116 **Supplementary Figure 1. Schematic illustrating *Tfp2a* and *Tfp2b* double conditional mutant genotypes**
 117 **depicting where *Tfp2a* and *Tfp2b* are deleted in the developing teeth in each tissue-specific cross. *Tfp2a* and**
 118 ***Tfp2b* are deleted in the ectoderm in *Cre^t* crosses (A, C) while in the *Wnt1-Cre* crosses, both genes are deleted in**
 119 **the neural crest-derived mesenchyme. Note that mesoderm-derived mesenchyme makes a minor contribution to the**
 120 **dental mesenchyme, shown here with a few colored mesenchyme cells that are *Wnt1-Cre* negative (B, D). In crosses**
 121 **utilizing conditional alleles for *Tfp2a* and *Tfp2b* (A, B), the *Cre*-negative tissues are “wild type” (green shading).**
 122 **In contrast, crosses that include *Tfp2a* and *Tfp2b* null alleles (C, D), *Cre*-negative tissues are heterozygous for**
 123 ***Tfp2a* and *Tfp2b* (blue shading).**



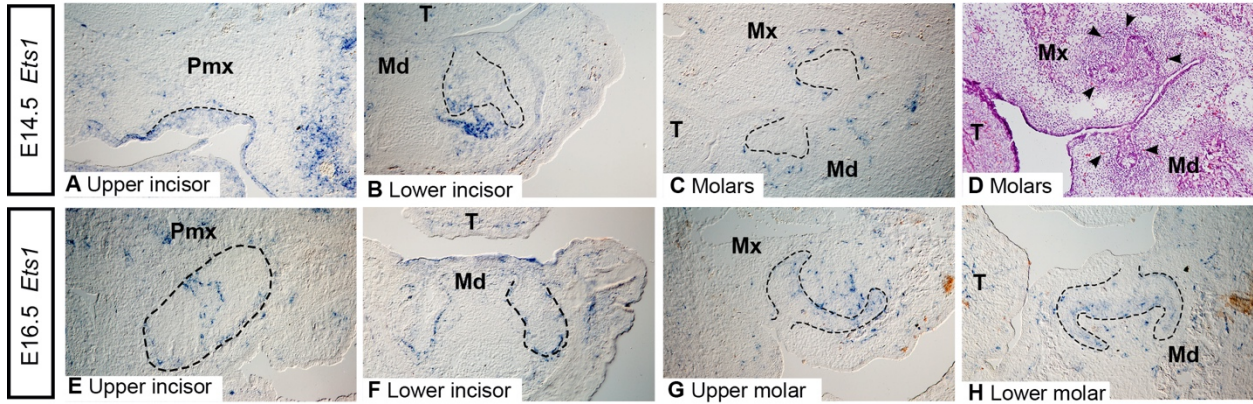
124
 125 **Supplementary Figure 2. Positive and negative controls for *in situ* hybridization for *Tfap2a*, *Tfap2b*, *Yeats4*,**
 126 ***Kctd1*, and *Ets1*.** Cryosections in the frontal plane showing that at E14.5 *Tfap2a*, *Yeats4*, and *Ets1* were detected in
 127 the eye (A-C), while *Kctd1*, and *Yeats4* were detected in the nasal epithelium (D, F) and *Tfap2b* was expressed in the
 128 nasal mesenchyme (E). *Tfap2b* was also expressed in the facial (surface) epithelium at E14.5 (G). Transcripts were
 129 not detected with the “sense” mRNA probes in frontal cryosections from molar tooth germs at E14.5 *Tfap2a* (H),
 130 *Kctd1* (J) *Ets1*, (L) or E13.5 *Tfap2b* (I), *Yeats4* (K). The molar epithelium is outlined in black. Note that only the
 131 right or left side of each frontal section is shown. Images taken of the embryos' right side (I, K, L) have been
 132 mirrored to match images taken of the left side. Images A-F, H-L taken at 10X, G taken at 5X. Mx: maxilla, Md:
 133 mandible, T: tongue.



134
 135 **Supplementary Figure 3. Frontal sections through bud stage (E13.5) incisors (A,B) and molars (C) showing**
 136 **CNCC-derived mesenchyme cells (EGFP-positive) labeled for three consecutive days via tamoxifen**
 137 **administration at E6.5-8.5 in *Sox10-iCre/ER^{T2};R26R^{mTmG/+}* or *Sox10-iCre/ER^{T2};R26R^{mTmG/mTmG}* embryos. The**
 138 **majority of dental mesenchyme cells are labeled with EGFP indicating that between ~E6.5 and 8.5 NCCs contribute**
 139 **extensively to incisor and molar tooth germs. The dental epithelium is outlined in white. Images taken at 20X. DE:**
 140 **dental epithelium, DM: dental mesenchyme.**

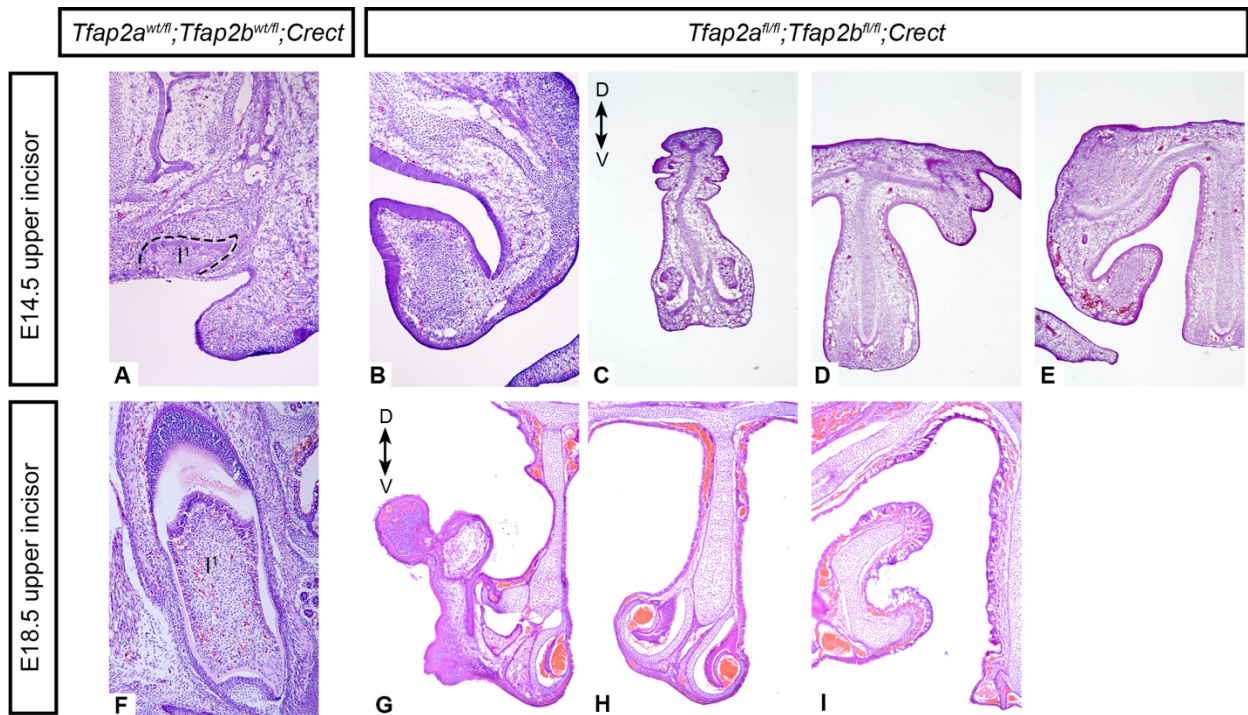


141
142 **Supplementary Figure 4. mRNA expression of *Yeats4*, and *Kctd1* at the late bud stage (E13.5, A-F) and cap**
143 **stage (E14.5, G-L).** mRNA transcripts detected by *in-situ* hybridization on frontal cryosections from the upper
144 incisor (left column), lower incisor (middle column), and molars (right column). Note that for both *Kctd1* and *Yeats4*
145 a stronger signal was detected at E14.5 than E13.5, predominantly in the dental epithelium but expression is also
146 present in the mesenchyme at the cap stage. At 14.5, the expression patterns of *Yeats4* and *Kctd1* are highly similar
147 to that of *Tfap2a* (Figure 2 M-O). Note that only the right or left side of each frontal section is shown. Images taken
148 of the embryos' right side (C, F, E, K) have been mirrored to match images taken of the left side. All images taken at
149 10X. Pmx: premaxilla, Mx: maxilla, Md: mandible, T: tongue.



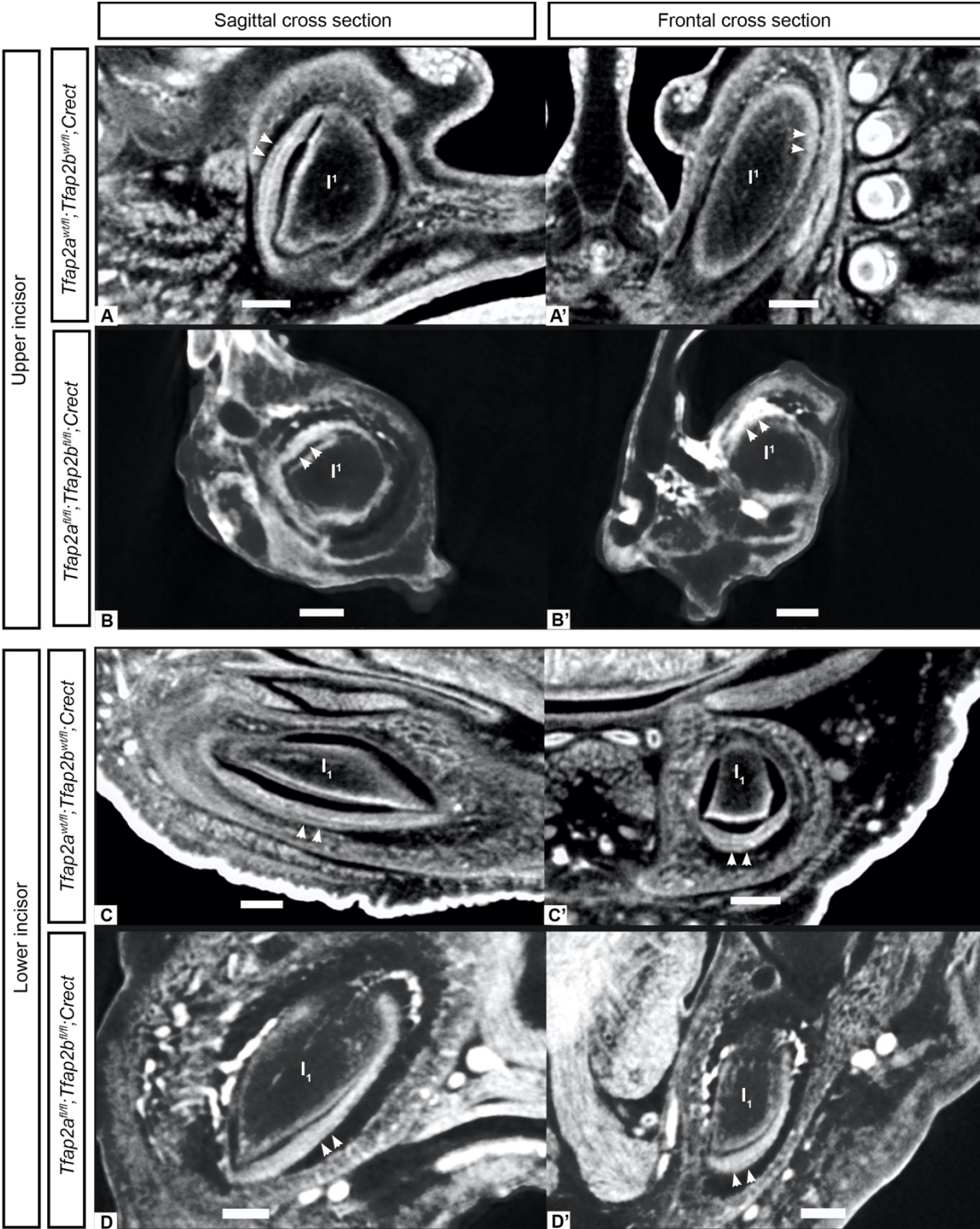
150
151
152
153
154
155
156
157
158
159

Supplementary Figure 5. Sparse, punctate expression of *Ets1* at the cap (E14.5) and early bell (E16.5) stages revealed by *in situ* hybridization. Cryosections in the frontal plane showing localization of mRNA transcripts of *Ets1* in incisor (A, B, E, F) and molar tooth germs (C, G, H). Note the similarity in the distribution of *Ets1* expressing cells (C) and red blood cells (D, arrowheads). Note that only the right or left side of each frontal section is shown. Images taken of the embryos' right side (E, G, H) have been mirrored to match images taken of the left side. Images taken at 10X. Pmx: premaxilla, Mx: maxilla, Md: mandible, T: tongue.

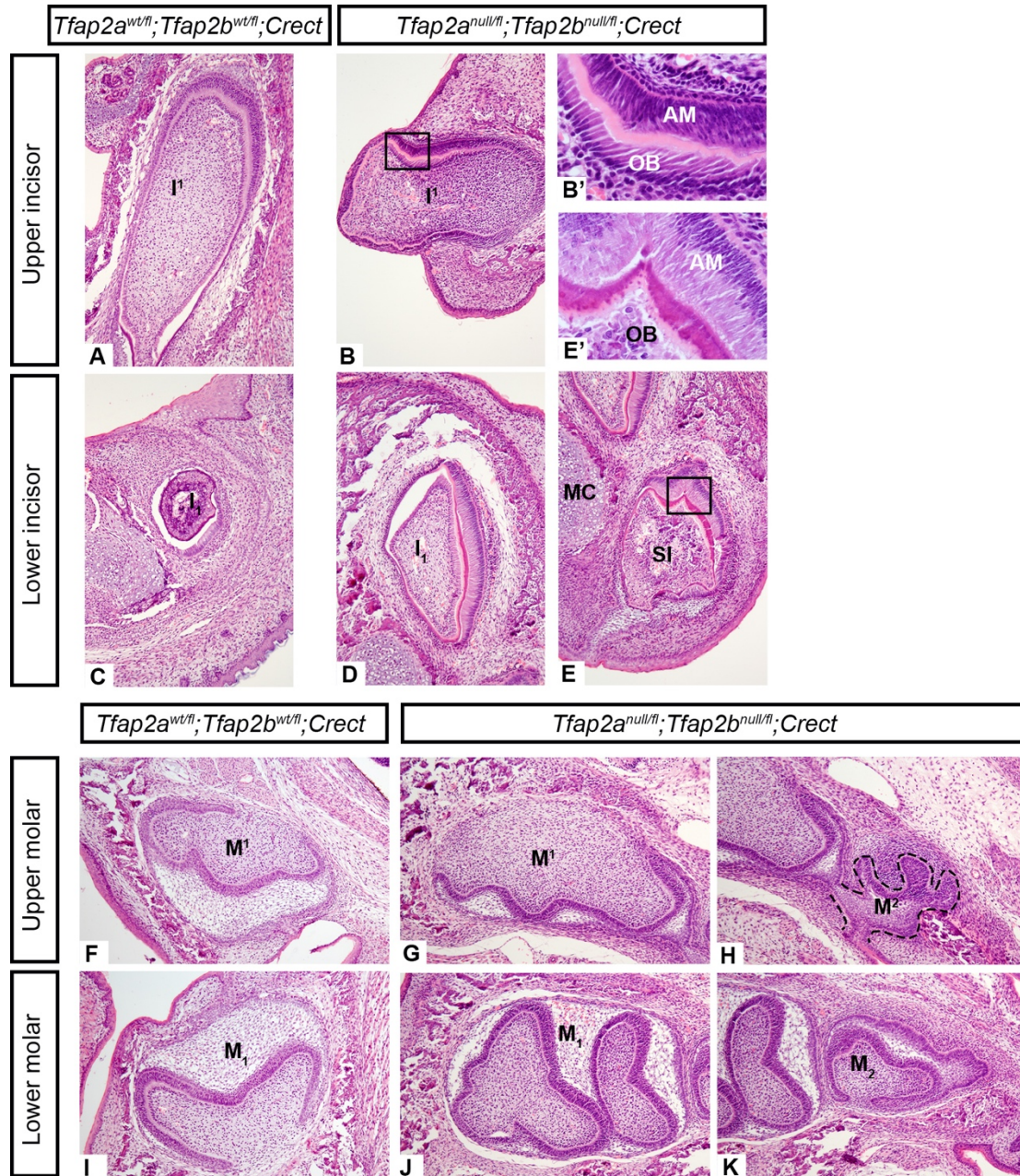


160
161
162
163
164
165
166
167
168

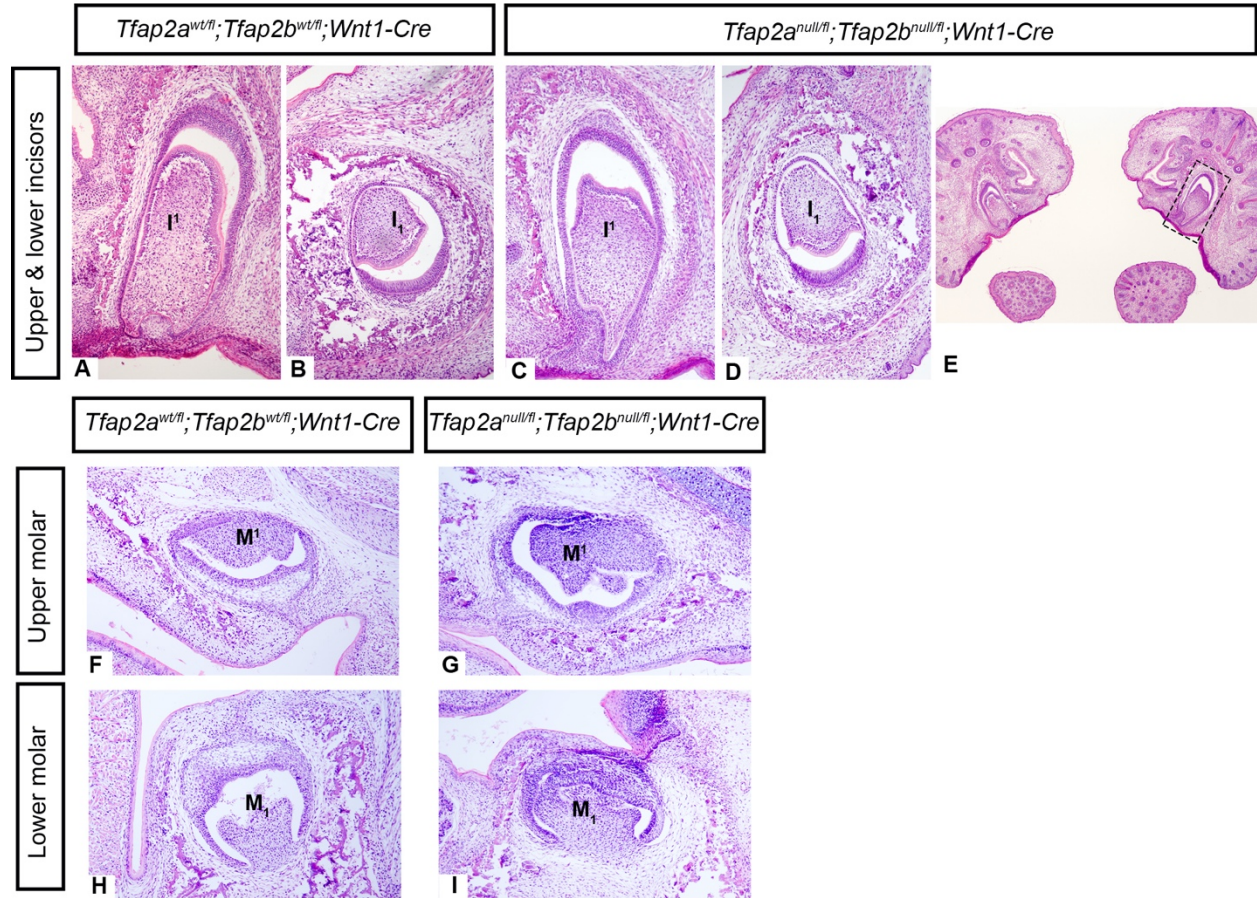
Supplementary Figure 6. Upper incisors are absent in some *Tfap2a*^{fl/fl};*Tfap2b*^{fl/fl};*Crect* embryos at E14.5 (B-E) and E18.5 (G-I). Histological sections in the frontal plane were stained with hematoxylin and eosin. Sections C-E and G-I are arranged with anterior-most sections on the left and more posterior sections on the right from the same individual embryos, respectively. Sections A (control) and B (mutant) are from comparable sectional planes along the anterior-posterior axis of the head. Note the right side of the E14.5 sections (A-E) and the left side of the E18.5 sections (F-I) are shown. Images A, B, F taken at 10X, C-E, G-I taken at 5X.



169
 170 **Supplementary Figure 7. Comparison of upper (A-B) and lower (C-D) incisors in control (A, A', C, C') and**
 171 ***Tfap2a^{nfl}; Tfap2b^{nfl}; Crect* mutant (B, B', D, D') embryos at E18.5. Sagittal (A-D) and lateral (A'-D')**
 172 **from μ CT data show the left upper or lower incisors, respectively. Note the whiter regions along the periphery of the**
 173 **tooth are the most dense and correspond to enamel (white arrowheads). Scale bars are 0.2mm.**



174
 175
 176 **Supplementary Figure 8. Comparison of the dentition in control (A, C, F, I) and mutant**
 177 **(*Tfap2a*^{null/fl};*Tfap2b*^{null/fl};*Cre*^t) embryos (B, D, E, G, H, J, K) show that upper incisors are present in the**
 178 **mutant (B) though the tooth is oriented horizontally as opposed to vertically in the control (A). Hematoxylin**
 179 **and eosin stained cryosections in the frontal plane showing that both upper and lower incisors are present in the**
 180 **control (A, C) and in the mutant (B, D). A ventral supernumerary incisor (E) is also present in the lower dentition of**
 181 **mutant embryos. Ameloblasts and odontoblasts are also present in the upper incisor (B, B') and in the**
 182 **supernumerary lower incisor (E, E') of the mutant. Molars in the mutant (G, H, J, K) appear similar to those of the**
 183 **control (F, I). Subtle differences in the shape of the mutant molars (G, J, H, K) and the apparent medial displacement**
 184 **of M^{2/2} relative to M^{1/1} (H, K) compared with those of the control (F, I) are due to a slightly offset plane of section**
 185 **resulting from the cleft palate and the mandible which is both clefted and downturned in the mutants (data not**
 186 **shown), as seen in the *Tfap2a*^{fl/fl};*Tfap2b*^{fl/fl};*Cre*^t mutants (Figure 4). Note that only the right or left side of each**
 187 **frontal section is shown. Images taken of the embryos' right side (A, C) have been mirrored to match images taken**
 188 **of the left side. Images A-K taken at 10X, B', E' taken at 40X. SI: supernumerary incisor, MC: Meckel's cartilage,**
 OB: odontoblasts, AM: ameloblasts.



189
 190
 191
 192
 193
 194
 195
 196
 197

Supplementary Figure 9. Teeth develop normally through the bell stage (E18.5) in mice lacking *Tfap2a* and *Tfap2b* in the neural crest derived mesenchyme (*Tfap2a^{null/fl};Tfap2b^{null/fl}; Wnt1-Cre*), despite clefting in the palate and mandible (E). Hematoxylin and eosin stained cryosections in the frontal plane showing that upper incisors (A, C) and lower incisors (B, D) appear similar in the mutant (C, D) compared to the control (A, B). Box in E surrounds upper incisor shown in C. Development of upper molars (F, G) and lower molars (H, I) also appears unperturbed in the mutant (G, I). Note that only the right or left side of each frontal section is shown. Images taken of the embryos' right side (A, B, F, H) have been mirrored to match images taken of the left side. Images A-D, F-I taken at 10X, image E taken at 5X.

198
199
200
201

Supplementary Table 1. Primer sequences for genotyping mice and embryos.

ND: not detected, NA: not applicable. Primers for *Sox10-iCre/ER^{T2}* mice obtained from: McKenzie, I.A., Ohayon, D., Li, H., de Faria, J.P., Emery, B., Tohyama, K., Richardson, W.D., 2014. Motor skill learning requires active central myelination. *Science* 346, 318–322. <https://doi.org/10.1126/science.1254960>

Target	Primer Sequence 5'-3'	T _m (°C)	Wild Type	Conditional	Mutant
<i>Sox10-iCre/ER^{T2}</i> Fwd (McKenzie et al. 2014)	TTGCGATGGGAGAGTCTGAC	64	ND	NA	742 bp
<i>Sox10-iCre/ER^{T2}</i> Rev (McKenzie et al. 2014)	AGGTACAGGAGGTAGTCCCTC				
<i>R26^{R^mTmG/mTmG}</i> Fwd (Endogenous) (JAX 8545)	AAAGTCGCTCTGAGTTGTTAT	64	558 bp	NA	337 bp
<i>R26^{R^mTmG/mTmG}</i> Rev 1 (Endogenous) (JAX 8546)	GGAGCGGGAGAAATGGATATG				
<i>R26^{R^mTmG/mTmG}</i> Rev 2 (Mutant) (JAX 7320)	TCAATGGGCGGGGGTCGTT				
<i>Tfap2a</i>	GCTCTCTCTTTTCCTGCCTTGGA ACCATGACCCTCAG	70	230 bp	265 bp	ND
<i>Tfap2a</i>	GTAACGTTGGCAGCTTTACGTC TCCCTGCTGGC				
<i>Tfap2b</i>	GTCTGTTTAGAACCTGGCTCAG CCAGAGGCTGG	70	210 bp	300 bp	ND
<i>Tfap2b</i>	CCCGAGCTAAGTGAACAGCTTC CCCTGTAAGGAGAGC				
<i>Wnt1-Cre</i>	GGAGCGTCCACTGGAGTCCAG GTCCTCTGGTTG	70	~310 bp	NA	~220 bp
<i>Wnt1-Cre</i>	CAAACCTAGGGTCATTAGACTTA CAAGGCATGTG				
<i>Wnt1-Cre</i>	CGCCAATACCCTACTCTTCCG GAGGAAAATGTC				
<i>Crect</i>	CCTCACTGATCCACATATGTCC TTCCGAAAGCTGC	68	586 bp	NA	385 bp
<i>Crect</i>	GATGCTAGAAAGCTGAGGCTG GGCTTAGCTTGCTAGGC				
<i>Crect</i>	CTACGCCGCGAACTTGCTTCTA GAGCG				

202

203
204

Supplementary Table 2. Dental phenotypes associated with different genotypes from *Crect* and *Wnt1-Cre* crosses.

Mutant or Control	Genotype	Stage	Affected Tissue	N	Dental Phenotype
Mutant	<i>Tfap2a^{fl/fl};Tfap2b^{fl/fl};Crect</i>	18.5 (bell)	Ectoderm (including dental epithelium)	4	Duplicated lower incisors (N=2/4) Ventrally-curved lower incisors (N=2/4) Upper incisors absent (3/4) Molars mesiodistally shortened (N=1)
Mutant	<i>Tfap2a^{fl/fl};Tfap2b^{fl/fl};Crect</i>	14.5 (cap)	Ectoderm (including dental epithelium)	3	Duplicated lower incisors (N=3/3) Upper incisors absent (N=3/3)
Mutant	<i>Tfap2a^{fl/null};Tfap2b^{fl/null};Crect</i>	18.5 (bell)	Ectoderm (including dental epithelium); <i>Cre</i> -negative tissues heterozygous for <i>Tfap2a/Tfap2b</i>	2	Duplicated lower incisors (N=2/2) One upper incisor absent (N=2/2)
Control	<i>Tfap2a^{fl/wt};Tfap2b^{fl/wt};Crect</i>	18.5 (bell)	None	3	Wild-type incisors and molars
Control	<i>Tfap2a^{fl/wt};Tfap2b^{fl/wt};Crect</i>	14.5 (cap)	None	3	Wild-type incisors and molars
Mutant	<i>Tfap2a^{fl/fl};Tfap2b^{fl/fl};Wnt1-Cre</i>	18.5 (bell)	Neural crest-derived mesenchyme	3	Wild-type incisors (N=3) and molars (N=2). Molars mesiodistally shortened (N=1). Cleft in midface (N=3)
Mutant	<i>Tfap2a^{fl/fl};Tfap2b^{fl/fl};Wnt1-Cre</i>	14.5 (cap)	Neural crest-derived mesenchyme	3	Wild-type incisors and molars
Mutant	<i>Tfap2a^{fl/null};Tfap2b^{fl/null};Wnt1-Cre</i>	17.5-18.5 (bell)	Neural crest-derived mesenchyme; <i>Cre</i> -negative tissues heterozygous for <i>Tfap2a/Tfap2b</i>	3	Wild-type incisors (N=3) and molars (N=2). Unknown if molars are mesiodistally shortened. Cleft in midface and mandible (N=3/3)
Control	<i>Tfap2a^{fl/wt};Tfap2b^{fl/wt};Wnt1-Cre</i>	17.5-18.5 (bell)	None	3	Wild-type incisors and molars
Control	<i>Tfap2a^{fl/wt};Tfap2b^{fl/wt};Wnt1-Cre</i>	14.5 (cap)	None	3	Wild-type incisors and molars

205
206
207
208

Supplementary Table 3. Primers used to amplify DNA sequences of target genes used for making mRNA probes for *in situ* hybridization.

Primer Name	Primer Sequence (5'-3')	Tm (°C)	Amplicon (bp)
<i>Tfap2a</i> Forward	GACCGTCACGACGGCACCAG	64	433
<i>Tfap2a</i> Reverse	GGACGTCCTCGATGGCGTGAG		
<i>Tfap2b</i> Forward	GCCTTGCTCTTACTGTGCAG	65	454
<i>Tfap2b</i> Reverse	CTATCTAGCTGCCCTTCGC		
<i>Ets1</i> Forward	GCTACGGTATCGAGCATGCTC	64	431
<i>Ets1</i> Reverse	CCAGGCACATGTTGTCTGGAG		
<i>Kctd1</i> Forward	GCATGTACTTCTGCACGCGAG	61	282
<i>Kctd1</i> Reverse	GCCGCTGGAAAAACGCCTTA		
<i>Yeats4</i> Forward	CAGAACTTGAAGTGAAAACCAG	54	315
<i>Yeats4</i> Reverse	TGGAGTCCTCTCTGAGAAAG		

209 **Supplementary Table 4. Upper and lower first molar measurements of wild mice and μ CT-scanned embryos.**
 210 Measurements (in mm) of molar occlusal surfaces of wild mice, *Mus musculus*, were obtained from Csanady, A.,
 211 Mosansky, L., 2018. Skull morphometry and sexual size dimorphism in *Mus musculus* from Slovakia. North-
 212 Western Journal of Zoology 14, 102–106. Measurements of control and mutant molars were obtained from μ CT
 213 scanned embryos from this study. Standard deviations for the mean measurements from the wild mice are also listed.
 214 The largest standard deviation (0.08, indicated with an asterisk) was used to estimate minimum and maximum
 215 values for molar length and width for the embryos examined in this study.

Tooth measurement	<i>Mus musculus</i>	<i>Tfap2a^{fl/wt}; Tfap2b^{fl/wt}; Crect (Control)</i>	<i>Tfap2a^{fl/fl}; Tfap2b^{fl/fl}; Crect (Mutant)</i>	<i>Tfap2a^{fl/wt}; Tfap2b^{fl/wt}; Wnt1Cre (Control)</i>	<i>Tfap2a^{fl/fl}; Tfap2b^{fl/fl}; Wnt1Cre (Mutant)</i>
Lower M1 mean length (mm)	1.34 +/- 0.06	1.043	0.857	1.157	0.718
Lower M1 mean width (mm)	0.78 +/- 0.03	0.577	0.558	0.590	0.508
Upper M1 mean length (mm)	1.61 +/- 0.08 *	1.210	0.953	1.297	0.926
Upper M1 mean width (mm)	0.98 +/- 0.04	0.636	0.613	0.665	0.611

216